AD-A093 745 NAVAL RESEARCH LAB WASHINGTON DC F/G 3/2
THE IONOSPHERIC RESPONSE TO SOLAR FLARES. I. EFFECTS OF APPROXI--ETC(U)
JAN 81 E S ORAN, J T MARISKA
UNCLASSIFIED NRL-MR-4428 NL

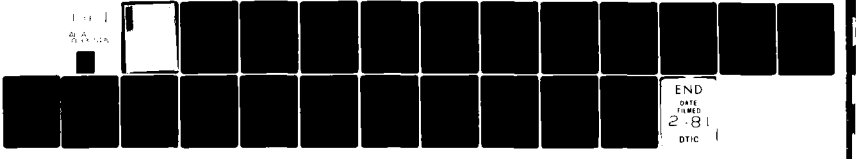

END
DATE FILMED
2-81
DTIC

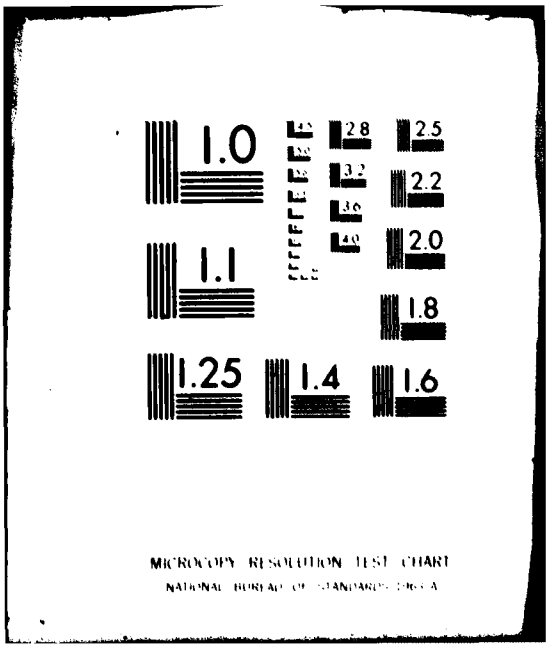
1.0
1.1
1.25
1.4
1.6
2.8
3.2
3.6
4.0
2.5
2.2
2.0
1.8
MICROCOPY RESOLUTION TEST CHART
NATIONAL BUREAU OF STANDARDS-1963-A

(16) RR033 02 (14) NRL-MK-4428

SECURITY CLASSIFICATION OF THIS PAGE (When Data Entered)

(9) **REPORT DOCUMENTATION PAGE**

READ INSTRUCTIONS BEFORE COMPLETING FORM

1. REPORT NUMBER NRL Memorandum Report 4428	2. GOVT ACCESSION NO. AD-A093745
3. RECIPIENT'S CATALOG NUMBER	
(6) 4. TITLE (and Subtitle) THE IONOSPHERIC RESPONSE TO SOLAR FLARES I. EFFECTS OF APPROXIMATIONS OF SOLAR FLARE EUV FLUXES	5. TYPE OF REPORT & PERIOD COVERED Interim report on a continuing NRL problem. 6. PERFORMING ORG. REPORT NUMBER
(10) 7. AUTHOR(s) Elaine S. Oran and John T. Mariska	8. CONTRACT OR GRANT NUMBER(s)
9. PERFORMING ORGANIZATION NAME AND ADDRESS Naval Research Laboratory Washington, DC 20375	(17) 10. PROGRAM ELEMENT, PROJECT, TASK AREA & WORK UNIT NUMBERS 61153N; RR0330244 44-0576-0-1
11. CONTROLLING OFFICE NAME AND ADDRESS Naval Research Laboratory Washington, DC 20375	(11) 16 12. REPORT DATE January 1981 13. NUMBER OF PAGES 22
14. MONITORING AGENCY NAME & ADDRESS(if different from Controlling Office) (12) 23	15. SECURITY CLASS. (of this report) UNCLASSIFIED 15a. DECLASSIFICATION/DOWNGRADING SCHEDULE

16. DISTRIBUTION STATEMENT (of this Report)

Approved for public release; distribution unlimited.

17. DISTRIBUTION STATEMENT (of the abstract entered in Block 20, if different from Report)

18. SUPPLEMENTARY NOTES

19. KEY WORDS (Continue on reverse side if necessary and identify by block number)

SOLRAD
Ionosphere
Solar flares
Aeronomy

20. ABSTRACT (Continue on reverse side if necessary and identify by block number)

SOLRAD and many other satellite systems have provided a large data base showing the time-dependent behavior of broad band solar fluxes in the X-ray and EUV spectral regions. These bands are broad in the sense that one band may contain many ionospherically important spectral lines. We present results of tests performed to determine how this information can best be used to predict the effects of a solar flare on the ionosphere. Our approach has been to first adopt a model of the spectral line and continuum enhancements based on a synthesis of many types of flare observations. This detailed spectral model is used in a time-dependent ionosphere model to calculate the response of the electron and ion density profiles. Then the spectral model is mathematically filtered to show how it would appear to the SOLRAD EUV detectors, and this degraded information is used in the

(Continues)

DD FORM 1 JAN 73 1473 EDITION OF 1 NOV 65 IS OBSOLETE
S/N 0102-LF-014-6601

251950 Plu

SECURITY CLASSIFICATION OF THIS PAGE (When Data Entered)

20. Abstract (Continued)

ionosphere model. Comparison of the two ionosphere calculations shows that the two spectra produces changes in the total electron content in the ionosphere that differ by only a few percent. More significant changes which occur in the individual species densities are described.

CONTENTS

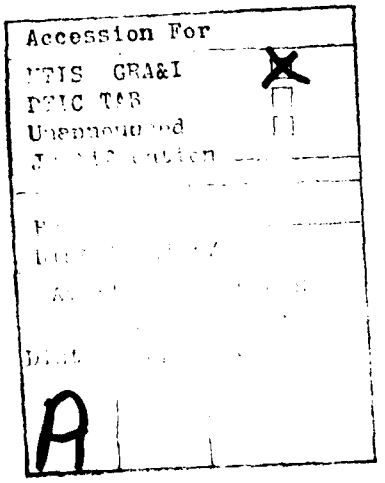

THE IONOSPHERIC RESPONSE TO SOLAR FLARES: I. EFFECTS OF APPROXIMATIONS OF SOLAR FLARE EUV FLUXES

INTRODUCTION

The increase in particle and electromagnetic radiation produced in a solar flare enhances the radiation impinging on the earth's atmosphere. These enhancements, which may vary dramatically from flare to flare, cause variations in the ionospheric electron density which in turn may have a major effect on the way in which radio and satellite communications systems function. Thus it is important to be able to assess quantitatively and in real time the effects of a solar flare on the earth's atmosphere.

The purpose of this paper is to present the first results of a study performed to determine how accurately we need to know the variations in X-ray and EUV emission accompanying a solar flare. Ideally we would like to start with knowledge of the behavior during a flare of all of the important individual lines and bands in the solar spectrum between about 1 and 2000 Å. Then this detailed information could be used as input to an ionospheric model which would then predict the ionospheric response. Unfortunately no flare has ever been observed in this detail, and the matter is further complicated by the fact that radiation enhancements due to flares can vary in intensity and energy distribution.

There exist, however, many time-dependent observations of broad spectral bands [e.g., Horan and Kreplin, 1980; Hinteregger et al., 1976] or of a limited number of emission lines [e.g., Wood et al., 1972; Hinteregger et al., 1976]. The work presented in this paper addresses the question of how the information in these data may be combined to model the effects of solar flares

Manuscript submitted November 3, 1980.

on the ionosphere. In particular, the use of SOLRAD 11 broad band EUV data [Horan and Kreplin, 1980] is examined.

Our approach to this problem has been to first adapt the detailed models of enhancements in the flare spectral intensity assembled by Donnelly [1976]. These spectra, which were assembled by a study of the existing data and represent a synthesis of many types of flare observations, were then used in to the NRL one-dimensional ionosphere model [Oran et al., 1974; Oran and Young, 1977] to calculate the time-dependent effects on the electron density profiles and the total electron content. Next we pass the detailed spectra through a mathematical filter to show how it would appear to the SOLRAD EUV detectors, and then use this degraded information in the ionosphere model. A comparison of the results obtained using the more detailed spectra to those obtained using the broad band spectra provides confidence in and a guide to the use of SOLRAD data for ionospheric modelling.

MODEL SPECTRA

The NRL one-dimensional model of the mid-latitude laminar ionosphere [Oran et al., 1974; Oran and Young, 1977] provides a detailed description of the ion, electron, and neutral densities and their respective temperatures as a function of time, altitude, and solar conditions. The model describes the heating of the ionosphere during the day by solar radiation and its maintenance at night due to the presence of resonantly scattered radiation and starlight [Strobel et al., 1976]. The solar radiation which is deposited at the top of the earth's atmosphere in the 1-2000 Å

range is divided into a number of bands. The criteria for the particular wavelength groupings chosen are that the calculated altitude profiles for ionization or dissociation must be within a few percent of those profiles produced when the full, detailed spectrum is used. The first two columns of Table 1 list the wavelength ranges of the bands used in the model and the quiet sun exospheric photon flux [Hinteregger et al., 1976; Donnelly and Pope, 1973] used in this study.

At each altitude at each time the ionization production rate of species i may be written as

$$q_i(z,t) = n_i(z) \sum_{\lambda} \sigma_i^{(i)}(\lambda)\phi_\infty(\lambda) \exp\left[- \sum_m \sigma_m^{(a)} \int_z^\infty n_m(s)ds \right], \quad (1)$$

where $q_i(z,t)$ is the photoionization rate of the i^{th} neutral species at altitude z, $n_i(z)$ is the density of the species at z, $\phi_\infty(\lambda)$ is the exospheric solar flux at wavelength λ, and $\sigma_i^{(i)}(\lambda)$ and $\sigma_i^{(a)}(\lambda)$ are the photoionization and photoabsorption cross-sections for species i for radiation at wavelength λ. Solar flares are simulated by varying in a prescribed manner the exospheric solar flux of each band to simulate the evolution of a solar flare.

The solar flare spectra proposed by Donnelly [1976] have both a fast and a slow component. Since we have found that the fast component has little effect on the electron density profiles or total electron content, we omit any discussion of this in the remainder of the paper. The slow component, however, could have major effects on those properties of the ionosphere which

affect communications systems [Oran et al., 1976].

The first step in adapting the slow-component model spectra was to renormalize the data. Donnelly adjusted the spectra so that the integrated energy was the same for each model spectrum he described. Thus the flares were differentiated by the photon or energy flux associated with a particular frequency range relative to the total flux in that spectrum. However, we also know that the integrated flux varies with the strength of the flare. Donnelly provided the unnormalized 1-8 Å flux and the relation between this flux and the 8-20 Å flux for each of the flares he tabulated. Thus we were able to use this information to scale the flare intensities appropriately. Next the spectra were used in conjunction with the quiet sun spectrum tabulated by Donnelly and Pope [1973] to calculate enhancement factors for the bands in the one-dimensional ionosphere model. The calculated enhancement factors for the two strongest flares tabulated by Donnelly are listed in Table 1. The first flare corresponds to an X25 class event and the second one to an X1 event.

The enhancements that would be seen by the SOLRAD detectors were calculated for the spectra described above by using the expression

$$E^{SOL}(\lambda_1-\lambda_2) = \sum_{\lambda_1}^{\lambda_2} \epsilon_\lambda \, F_\lambda\,(D) \;\Big/ \sum_{\lambda'}^{\lambda_2} \epsilon_\lambda \, F_\lambda\,(QS). \qquad (2)$$

Here the numerator represents the convolution of the flare spectrum with known SOLRAD detector efficiencies. The denominator is a normalization factor derived from convolving the quiet sun spectrum

TABLE 1. Model Spectra

Band	Quiet Sun Flux (photons cm^{-2} s^{-1})	Enhancement (Detailed)		Enhancement (SOLRAD)	
		X25	X1	X25	X1
1-3	1.00(1)*	2000.	2000.	2000.	2000.
3-5	2.00(3)	60.	60.	60.	60.
5-10	1.50(5)	40.	40.	40.	40.
33.6	3.50(7)	30.8	4.98	30.8	4.98
40-50	6.60(7)	9.16	3.24	9.16	3.24
50-60	1.67(8)	9.16	3.24	9.16	3.24
60-80	2.10(8)	7.98	2.16	7.98	2.16
80-100	3.30(8)	7.98	2.16	7.98	2.16
100-205	5.10(9)	3.45	1.44	2.15	1.21
205-370	7.60(9)	2.19	1.22	2.15	1.21
335 lines**	7.21(9)	1.25	1.05	2.15	1.21
370-630	5.33(9)	1.25	1.05	1.25	1.05
630-800	2.41(9)	1.25	1.05	1.52	1.08
800-911	2.90(9)	1.99	1.15	1.80	1.12
860-911	6.03(9)	1.99	1.15	1.80	1.12
911-1027	2.30(9)	1.43	1.08	1.80	1.12
972.5	8.00(8)	1.43	1.08	1.80	1.12
977,990	5.00(9)	1.43	1.08	1.80	1.12
1025.7	3.50(9)	1.43	1.08	1.80	1.12
1027-1310	1.75(10)	1.43	1.08	1.80	1.12
1215.7	3.00(11)	1.43	1.08	1.80	1.12

*Read 1.00(1) as 1.00×10^{1}

**Band consists of the emission lines at 308.8, 335.4, 360.7, 364.8, and 368.1 Å.

with the SOLRAD detector efficiencies. The efficiencies for the SOLRAD detectors are shown in Figure 1. Also plotted on the figure is the Donnelly and Pope [1973] solar spectrum. The results of these calculations for the two strongest flares tabulated by Donnelly are listed as the last two columns in Table 1.

Table 1 shows the effect of the smoothing by the SOLRAD detectors. These differences may be understood by referring to Figure 1 which shows that the detectors have their highest efficiency in the shorter wavelength regions of their band pass and then decline at longer wavelengths. This means that the flare enhancements for each band are weighted toward the short wavelength portion of the band. Since in general flares have larger enhancements at shorter wavelengths, there will be a tendency to add too much flux to the NRL ionosphere model bands that fall in the long wavelength region of each SOLRAD band. The wavelength regions from 370-630 Å and above 911 Å show this effect in Table 1. There will also be some reduction of the flux at shorter wavelengths in each band.

Solar flares exhibit a wide range of time scales for the slow component. For this study we have assumed that the flare is characterized by an exponential rise, followed by a constant phase, followed by an exponential decline. Although there is some tendency for shorter wavelengths to rise before longer wavelengths, we have used the same times for all bands in the model. For the rise we use a duration of 7 minutes, for the constant phase a duration of 5 minutes, and for the decay a duration of 20 minutes. Figure 2 shows the time profile for the enhancement in a typical

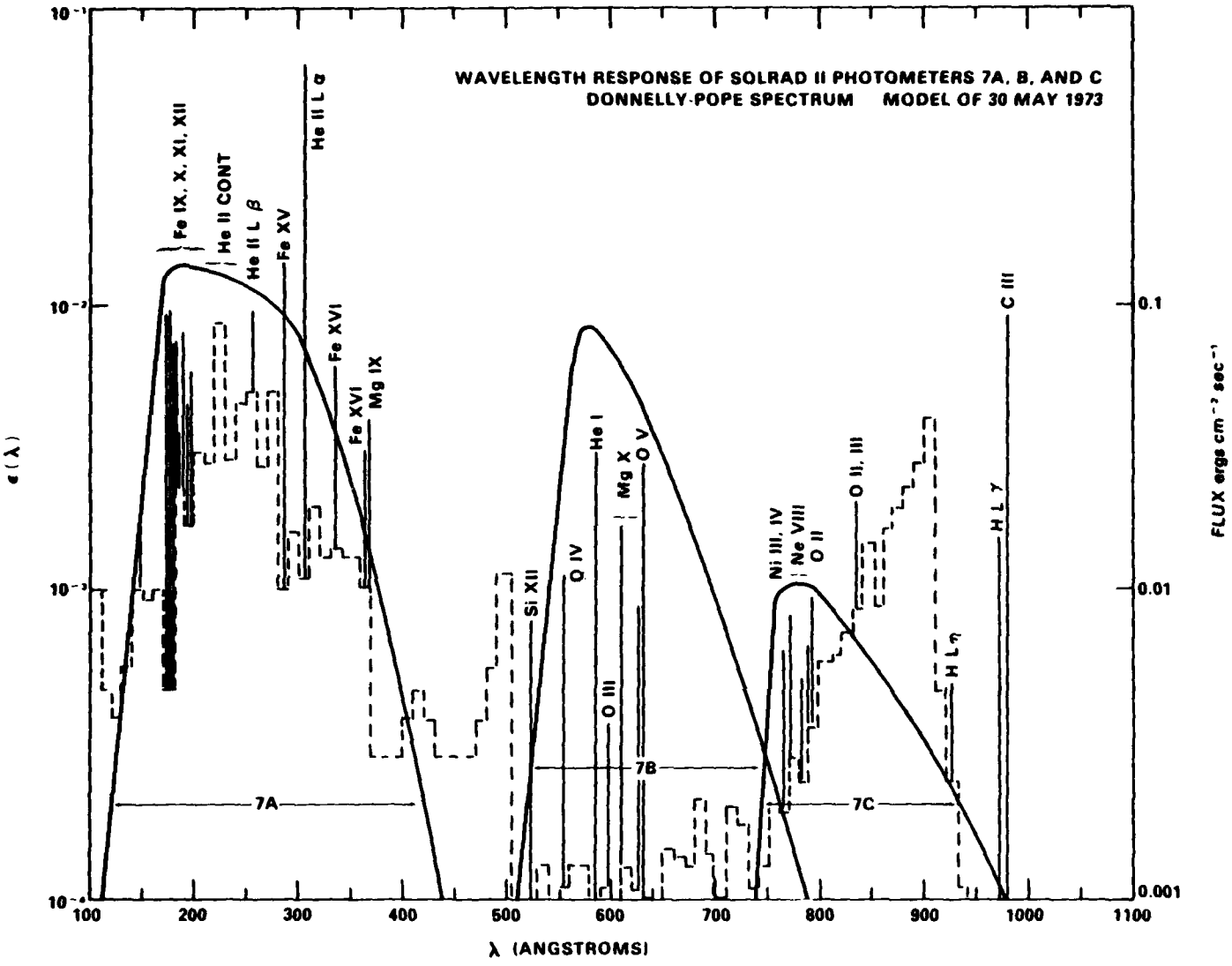

Fig. 1 - The heavy solid lines show the wavelength response of the SOLRAD 11 photometers. The background quiet sun spectrum (dashed lines and thin solid lines) is taken from Donnelly and Pope (1973).

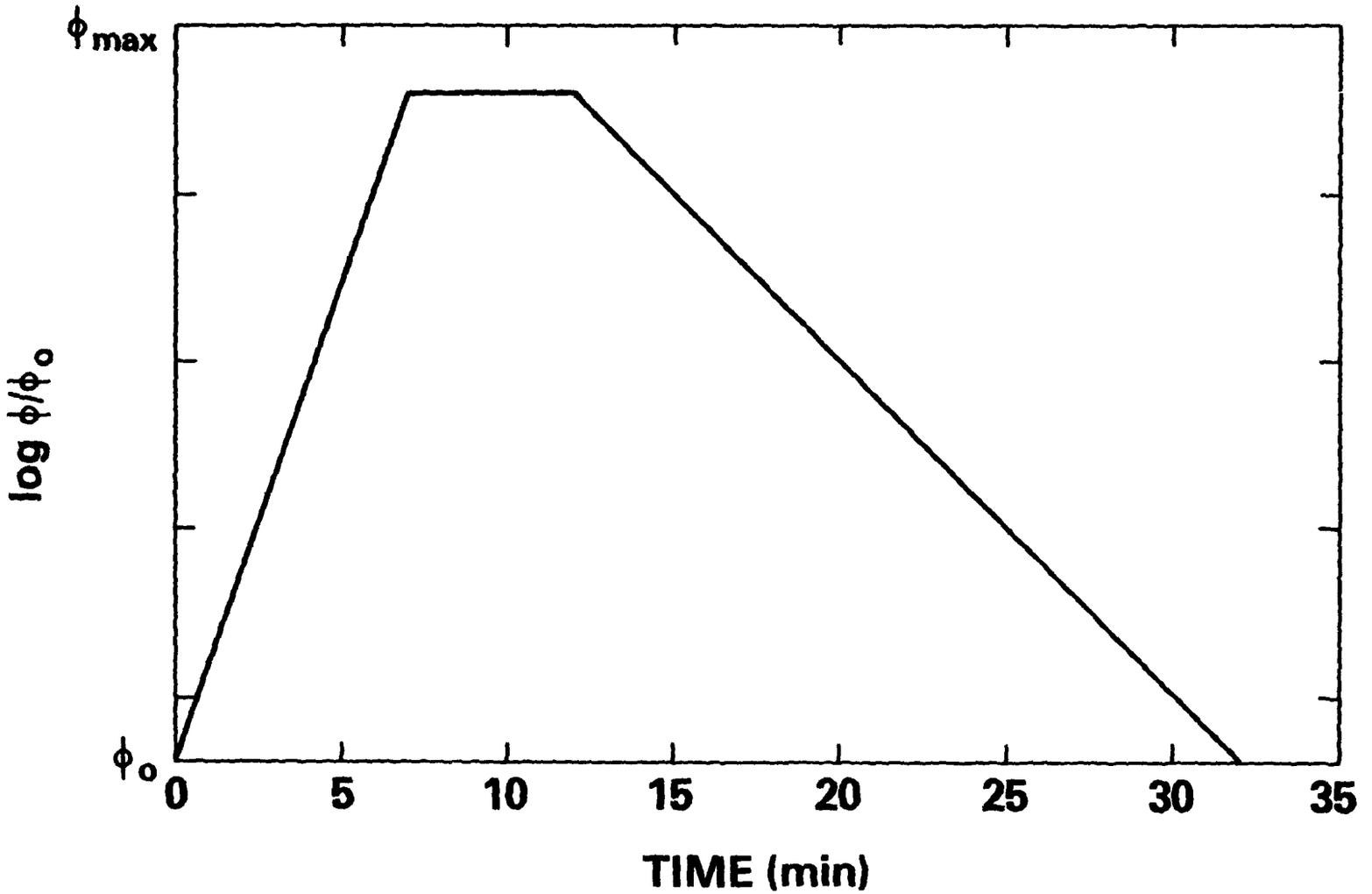

Fig. 2 - Time-profile for the enhancement of the solar radiation due to a solar flare, where ϕ is the exospheric flux and ϕ_{max} is the peak value that flux achieves during a flare

band. Since we are primarily interested in the EUV region of the spectrum, we have used the same fluxes in the detailed model and the SOLRAD model for all of the bands below 100 Å.

RESULTS

One commonly measured indication of the state of the ionosphere is the total electron content, N_T. Figure 3 shows calculations of N_T as a function of time for the two flares listed in Table 1 for flares beginning at noon. The solid lines result from the detailed flare spectra used directly in the ionosphere model, while the dashed lines result from convolving the flare spectra with the SOLRAD detector efficiencies and using this input in the ionosphere model. The figure indicates that using the SOLRAD data makes only a small difference in the calculated values of N_T. For the strongest flare, this difference is about 4%.

Figure 4 shows electron density contours corresponding to the quiet sun and both models of the X25 flare. Noticeable perturbations in electron densities occur at altitudes below 350 km. The largest change in density occurs at about 200 km, which is also the altitude range for which there is a significant increase in the electron densities produced by the detailed spectrum over those produced by the SOLRAD spectrum.

To understand the source of this difference it helps to examine contour plots of the principal ions formed in this region. Figures 5 and 6 show contour plots of the number densities of O^+ and O_2^+, respectively. These figures indicate that the primary source of the additional electrons in the calculation using the detailed model is the increase in O^+ around 200 km,

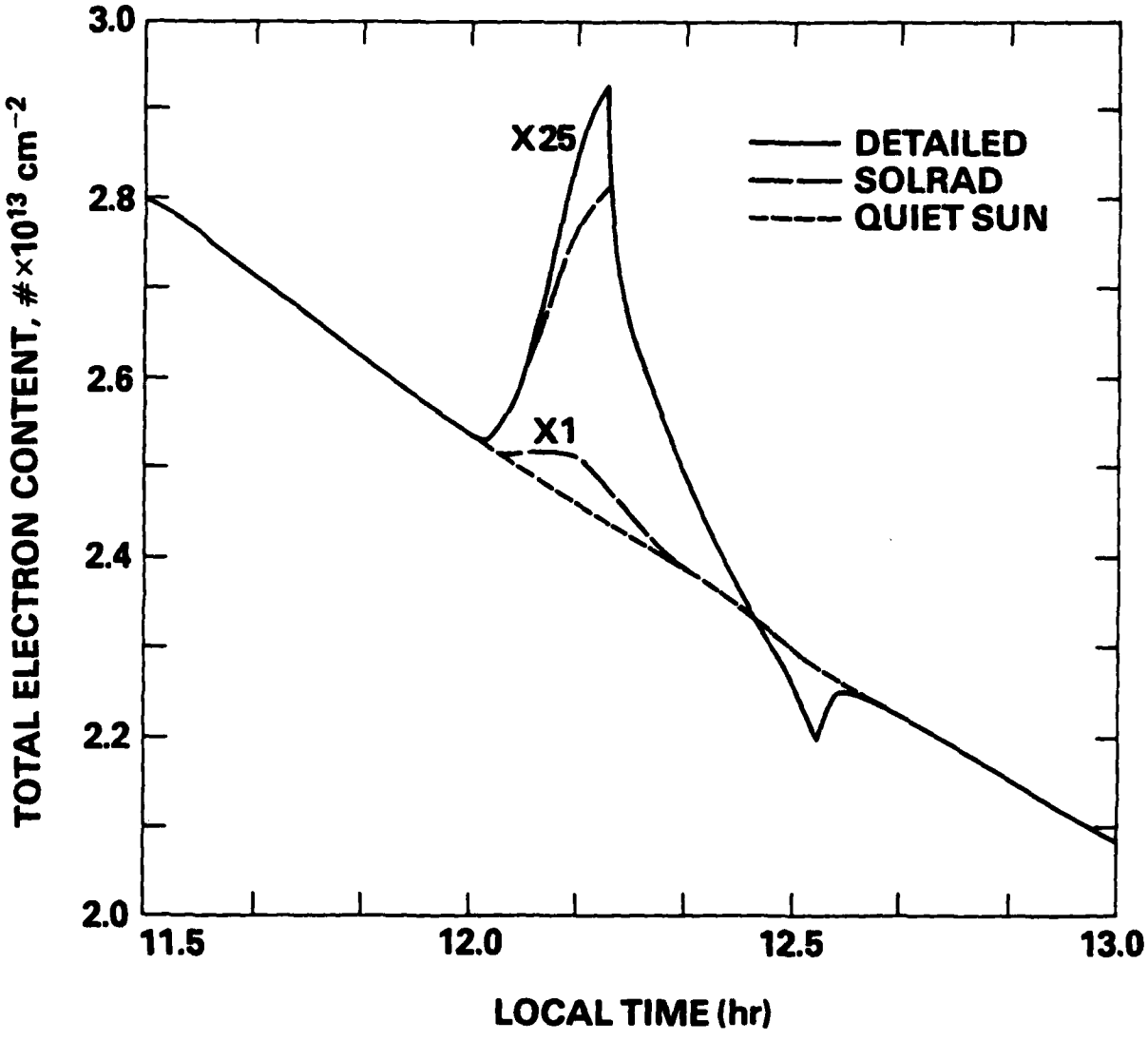

Fig. 3 - Comparison of calculations of total electron content using the detailed spectra and the SOLRAD spectra for an X25 and X1 flare

with some additional contribution from increased O_2^+ at about 150 km. At 200 km radiation in the 100-205 Å band provides the primary source of photons for photoionization of atomic oxygen. Thus the approximately 38% difference in the flux in this band between the Donnelly spectra and the SOLRAD spectra accounts for the additional O^+ and the additional N_T.

Figures 4 through 7 also show that two regions of perturbation occur before the atmosphere relaxes to the unperturbed state. The first is one in which the electron density is increased relative to the quiet sun values due to direct ionization by the enhanced solar flux. An increase in electron temperature is also noted during this period due to the enhancement of the ion production rates. Enhanced temperature and enhanced direct production of O^+ and O_2^+ lead to an enhancement in NO^+, as shown in Figure 7. This period is followed by one in which the electron density is decreased relative to quiet sun values due to increased recombination rates with increasing temperature. These processes finally relax to nonperturbed values by 13:00 LT.

CONCLUSIONS

The results presented have focused primarily on the calculations representing the response of a quiet, mid-day ionosphere to an X25 flare with a photon distribution given in Table 1. Our calculations have shown that this flare produces a maximum deviation in total electron content of about 12% (Figure 3) with a substantial part of the added ionization occurring above the F2 peak (Figure 4). The most dramatic deviations occur below 200 km, where we first see

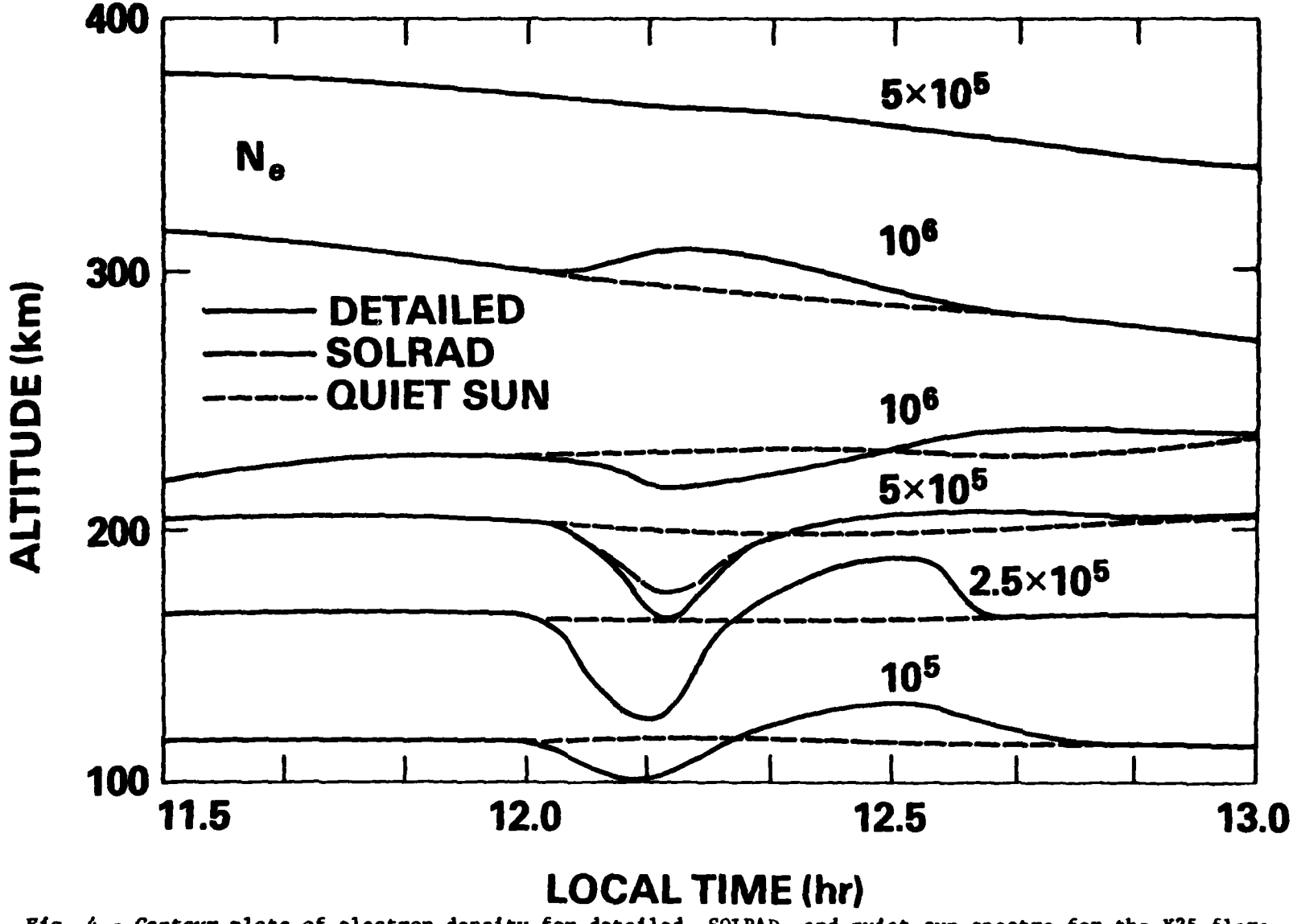

Fig. 4 - Contour plots of electron density for detailed, SOLRAD, and quiet sun spectra for the X25 flare

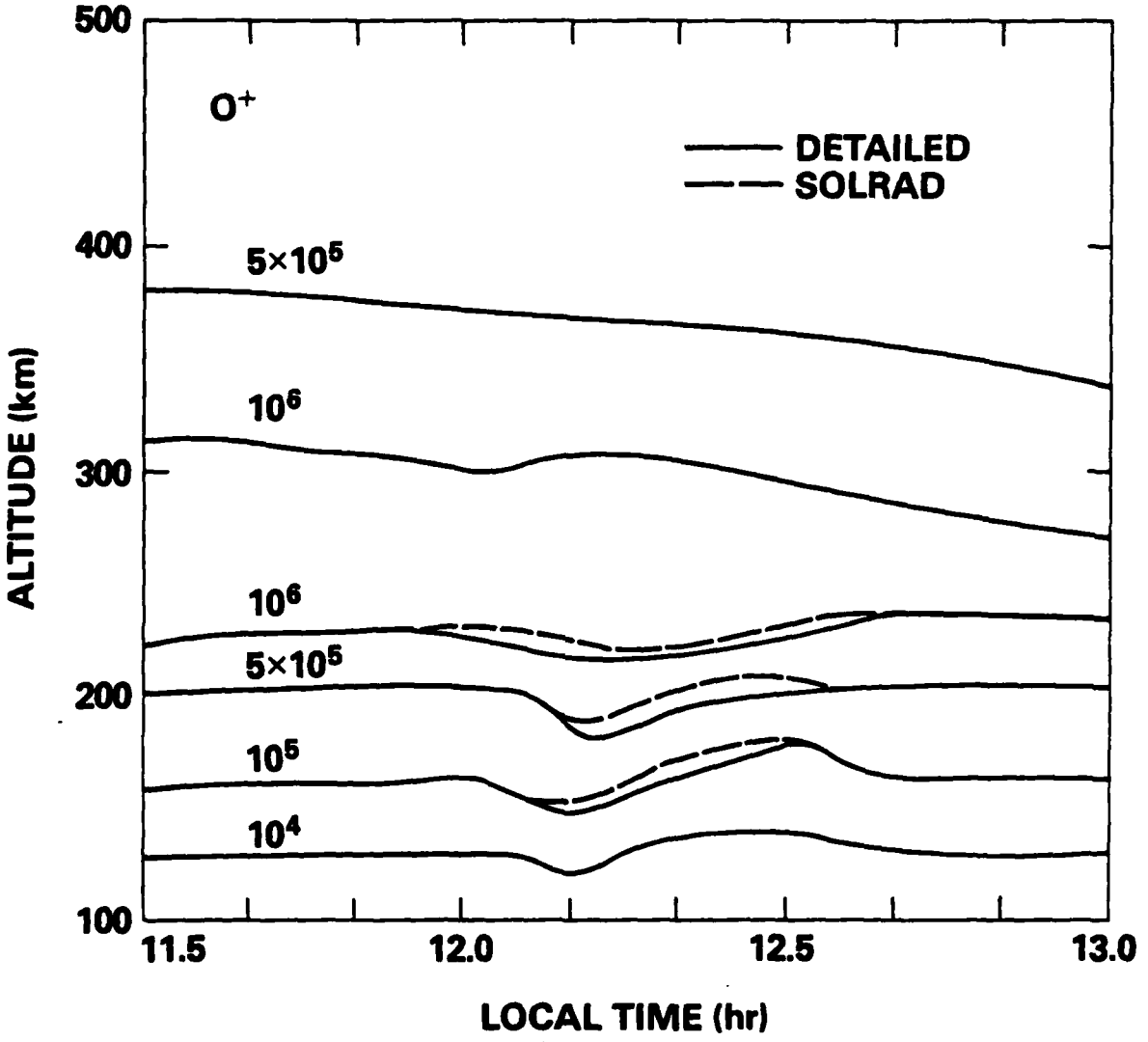

Fig. 5 - Contour plots of (O^+) for detailed SOLRAD, and quiet sun spectra for the X25 flare

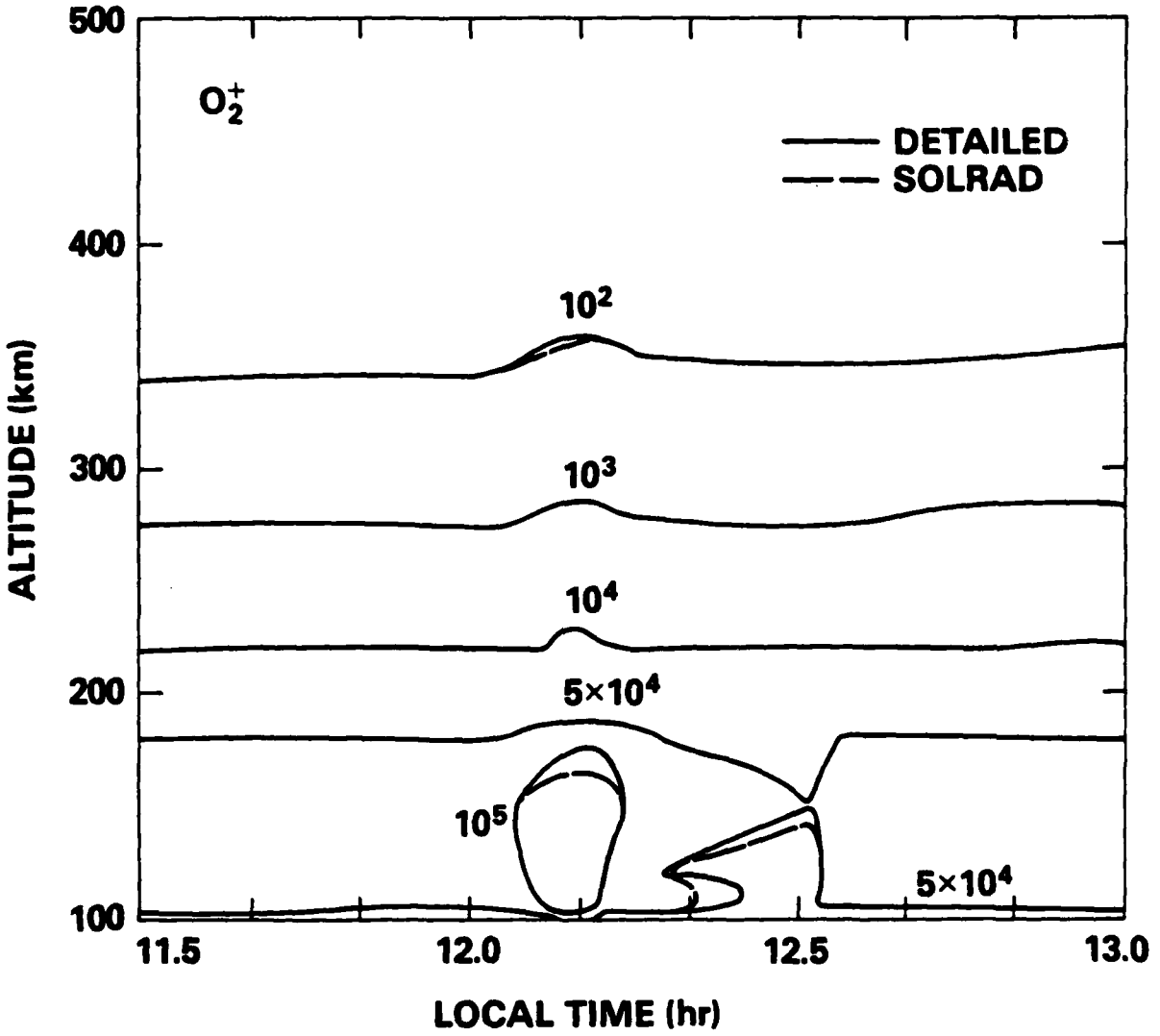

Fig. 6 - Contour plots of (O_2^+) for the detailed and SOLRAD spectra for the X25 flare

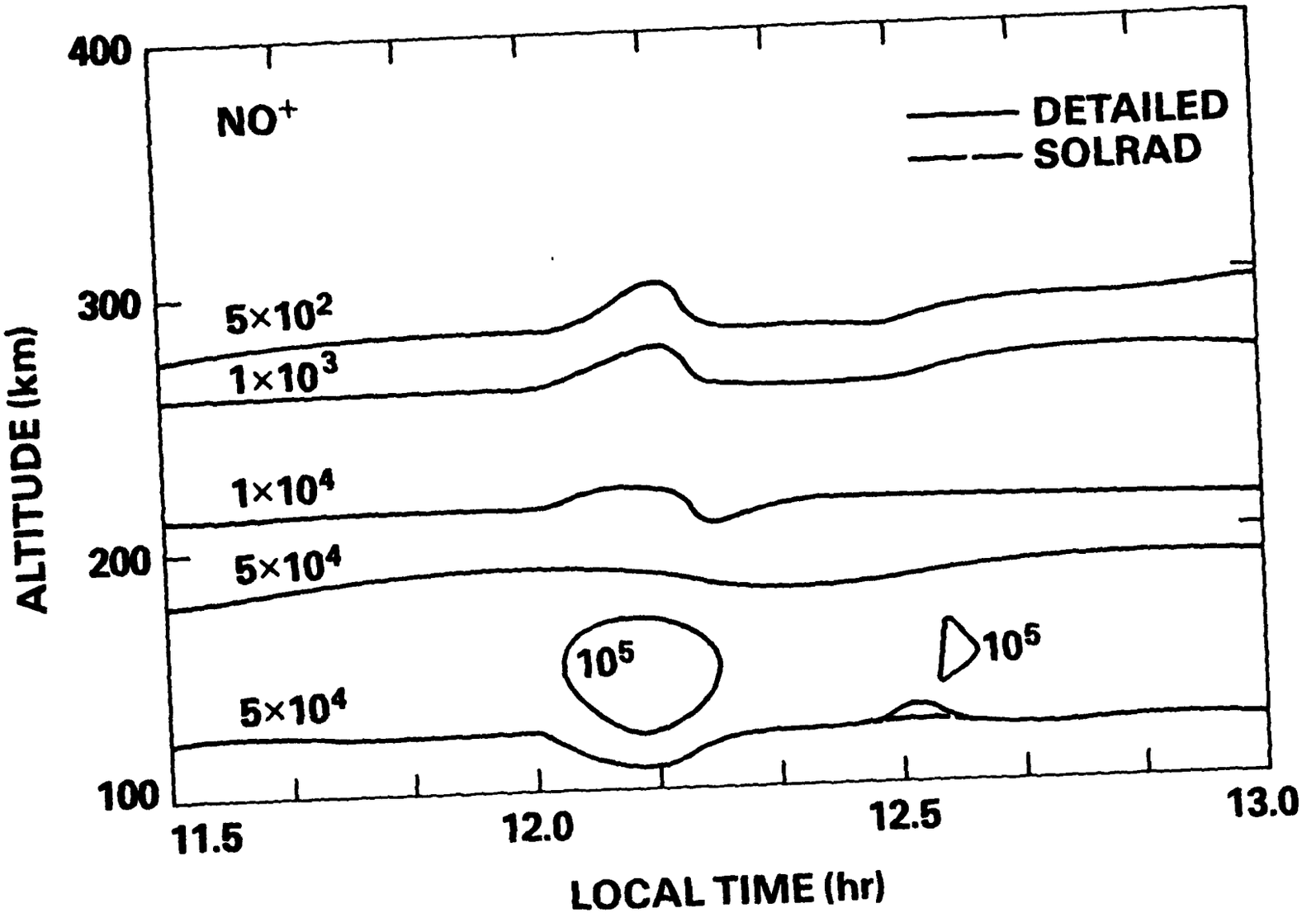

Fig. 7 - Contour plots of (NO^+) for the detailed and SOLRAD spectra for the X25 flare

an ionization enhancement due directly to the increase of solar radiation. Then the effects of increased electron temperature take over and increase the recombination rates and the chemical reaction rates leading to NO^+ production (Figures 4 to 7). For the particular flare chosen, which produces enhanced radiation for about a half hour, we observe that it takes the ionosphere another half hour to totally relax.

The major purpose of this paper is to compare the results of a detailed flare model to those of a flare that SOLRAD 11 would detect. This comparison has been very encouraging both in the integrated features, such as total electron content (Figure 3), and in the details of the ionospheric profiles, such as Ne, O^+, O_2^+, and NO^+ (Figures 4 to 7). The major deviations between the two calculations of this flare occur below 200 km and are due to the way in which we filter the 100-205 Å band. The results have led us to believe that a series of studies such as this one could lead to a set of empirical correction factors for the bands used in the ionosphere model given certain types of flares. What is certainly needed now is data for several real flares which are at least as detailed as the hypothetical flare Donnelly constructed. Then much more reliable empirical corrections could be obtained for input to ionosphere models.

Our future work will proceed in two directions. First, we will apply information such as we have derived above to specific flares observed by SOLRAD. Second, we will study in detail the effects of increased ambient electron heating efficiency due to the enhanced ionization.

ACKNOWLEDGEMENTS

This work has been sponsored by the Naval Research Laboratory through the Office of Naval Research. The authors would like to acknowledge helpful conversations with Drs. Ted Young, Uri Feldman, George Doschek, R. Kreplin, and D. Horan. The authors would also like to thank Drs. A. Berman and H. Rabin for inspiring the interactions which led to this work.

REFERENCES

Donnelly, R.F., Empirical models of solar flare X-ray and EUV emission for use in Studying their E and F region effects J.Geophys. Res., 81, 4745-4753, 1976.

Donnelly, R.F., and J.H. Pope, The 1-3000 Å solar flux for a moderate level of solar activity for use in modelling the ionosphere and upper atmosphere, Tech. Rep. ERL 276-SEL25, NOAA, Boulder, Colo., 1973.

Hinteregger, H.E., D.E. Bedo, J.E. Manson, and D.K. Skillman, EUV Flux variations with solar rotation observed during 1974-1976 from AE satellites C, D, and E, Space Res., XVII, 533, 1976.

Horan, D.M., and R.W. Kreplin, Measurements of solar EUV and soft X-ray emission during sudden frequency deviations, J. Geophys. Res., 85, 4257-4269, 1980.

Oran, E.S., T.R. Young, D.V. Anderson, R.P. Coffey, P.C. Kepple, A.W. Ali, and D.F. Strobel, A numberical model of the mid-latitude ionosphere, NRL Memo 2839, Nav. Res. Lab., Washington, D.C., 1974.

Oran, E., L. Baker, and T.R. Young, The effects of solar flares on the ionosphere, NRL Memo 3296, Nav. Res. Lab., Washington, D.C. 1976.

Oran, E.S., and T.R. Young, Numerical modelling of ionosphereic chemistry and transport processes, J. Phys. Chem., 81, 2463-2467, 1977.

Strobel, D.F., T.R. Young, T.P. Coffey, and A.W. Ali, The Nighttime Ionosphere: E Region and Lower F Region, J. Geophys. Res., 79, 3171, 1974.

Wood, A.T., Jr., R.W. Noyes, A.K. Dupree, M.C.E. Huber, W.H. Parkinson, E.M. Reeves, and G.L. Withbroe, Solar flares in the extreme ultraviolet, 1, The observations, Solar Phys., 24, 169-179, 1972.